*Transactions*, SMiRT-26
Berlin/Potsdam, Germany, July 10-15, 2022
Division IV

# VALIDATION OF EARTHQUAKE-INDUCED ROCK COLLAPSE ANALYSIS BY SIMPLIFIED DEM MODEL FOR EVALUATION OF TRAVELING DISTANCE AND SEDIMENTAION STATE

**Hitoshi Nakase[1] and Yukio Nakata[2]**

[1] Specialist, Tokyo Electric Power Services co. ltd, Tokyo, Japan (nakase@tepsco.co.jp)
[2] Professor, Yamaguchi University, Ube, Yamaguchi, Japan

## ABSTRACT

A nuclear facility safety assessment needs to estimate the risk of a stronger earthquake than originally envisioned in the design. Nakase et. al. (2015) proposed and validated a simple model using the discrete element method developed Cundall(1971) to evaluate the traveling distance of a collapsed rock mass when slope collapse occurs. Here, further validation was repeated by performing a reproduction analysis of a rock for experiments on a full-scale slope. Then, a concrete method for evaluating the sedimentary behaviour of rocks was proposed.

## INTRODUCTION

Our purpose is to predict the sedimentary state of the collapsed rocks as shown in Fig. 1 by numerical simulation when the slope collapses. It is easy to think that this prediction is impossible due to the large number of uncertainties. However, the sedimentation behaviour of rocks is more reproducible than expected.

Figure 1. Bedrock collapse of Erimo-cho in 2004

Figure 2 shows flow experiment of 0.5 cubic meters of crushed stone performed by Nakamura et. al. (2018). The difference in reach of the tips of the crushed stones that ran down the slope covered with a 6.2 m high concrete slab twice was only 6 cm as shown in Figure 3. This indicates that the sedimentary behaviour is predictable once the slope shape and the physical characteristics of the rock are determined. But, the problem is how to set the physical characteristics of the rock during collapse. In this study, we will explain about how to solve this problem.


Figure 2. Crushed stone 0.5 cubic meter flowing experiment

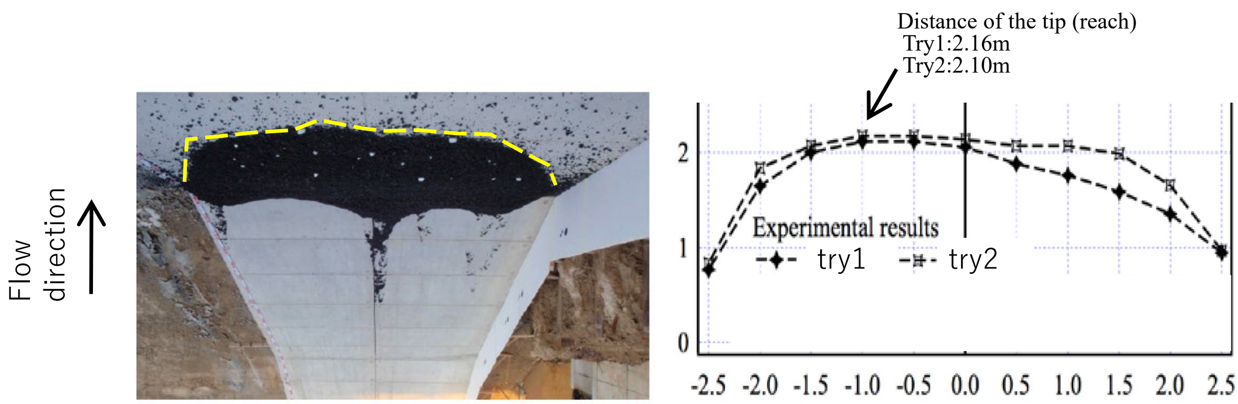


Front line of sediment (yellow dashed line) Front lines of the two experiments

Figure 3. Difference between two experiments

**REPULSION EXPERIMENT OF ROCK**

The main factors that complicate the slope failure phenomenon are the repulsion between rocks and slopes and the repulsion between rocks and rocks. The stronger this repulsion, the greater the variability. However, the larger the rock, the smaller the repulsion. Here, we will explain the results of the vertical drop test of the specimen a rock of a size that is likely to cause damage.

Figure 4 shows the state of the experiment. A test piece with a mass of 3 t was dropped vertically from a height of 5 m onto asphalt pavement. This test piece corresponds to a rock with a diameter of 1.3 m assuming a density of 2600 kg / m$^3$. The specimen had little repulsion. The degree of repulsion of the specimen depends on the opponent it collides with. Concrete pavement is considered to be the most repulsive on the site of the power plant. Figure 5 shows the results of a vertical drop test on a concrete slab with a thickness of 1 m. The coefficient of restitution is the velocity ratio before and after the collision. The heavier the mass of the specimen and the higher the drop height, the smaller the coefficient of restitution. The coefficient of restitution for concrete slabs is higher than that for concrete pavement, but it is still at most 0.3. A collision with a coefficient of restitution of 0.3 consumes 90% of the kinetic energy. The coefficient of restitution of the collapsed rock is an uncertain factor, but it can be said that the possible range is about 0.3 or less.

Initial state — Immediately after the collision

Figure 4. Vertical drop test of specimen (asphalt pavement)

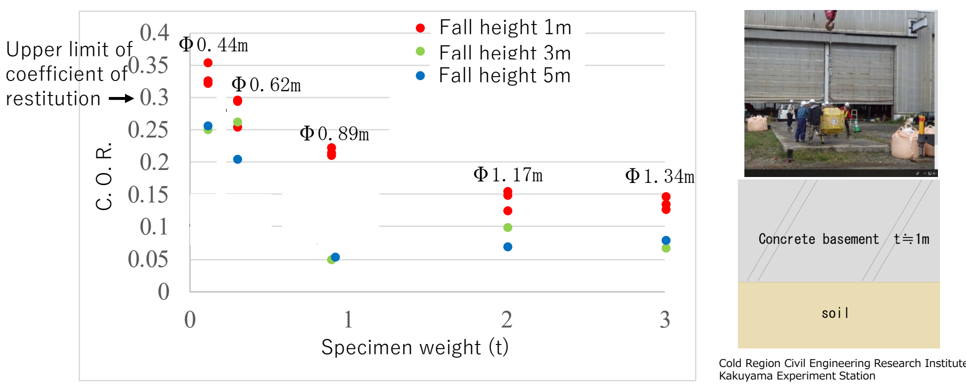


Figure 5. Coefficient of restitution against concrete slab

## ROCK FALL EXPERIMENT AND REPRODUCTION ANALYSIS

Immediately before the sedimentation immediately after the slope collapses, there should be a phenomenon in which individual rocks repeatedly collide with and roll on the slope and the ground. Therefore, it is important that the proposed method demonstrates the ability to reproduce the behaviour of a single rock rolling down a slope and rolling on the ground.

An experiment was conducted in which iota type test piece with three different weights were dropped from a height of 25 to 30 m onto the slope. Figure 6 shows the experimental site and the test piece that is a model of the rock. Since this is a place to mine sand, the slope and the ground are after excavated sandstone. Figure 7 shows a cross-sectional view of the experiment. The gradient of slope is 53 degrees. The edge of the pit is a cliff, and a protective equipment was installed to prevent the specimen from falling. The distance from the slope to the protector is 39m. Figure 8 shows the floor plan. Two types of pavement were applied to the area where the test piece rolled down the slope and landed on the ground in a range of 15 m in length and 6 m in width. Specimens released from four locations rolled on the slope approximately along the lane shown in Figure 8, bounced on the catwalk shown in Figure. 6, and incident toward the ground. Then, 25 out of 33 test pieces, 75%, fell on the paved ground. The height of the release point was 30m in lane1 and 25m in other lanes. The moment the specimens collided with the ground were taken with a high-speed cameras. The apparent coefficient of restitution of the first bounce was 0.38 for asphalt pavement and 0.34 for concrete pavement, and there was almost no difference between the two. The apparent coefficient of restitution is the velocity ratio in the vertical direction when obliquely incident, and tends to be larger than the coefficient of restitution when vertically dropped. As shown in Table 1, there was almost no difference in the incident conditions between the two in the cross section plane. Here, the rotation ratio is the rotation angular velocity of the test piece divided by the radius and the incident velocity. When rolling down a frictional slope, it is considered that the closer the test piece is to a sphere, the closer the rotation ratio is to one. The specimen rolling on the ground was photographed using a drone in the sky. The trajectory will be compared later with a numerical simulation.


Experiment site

EOTA type test piece (1.6t in this picture)

Figure 6. Rock Fall Experiment

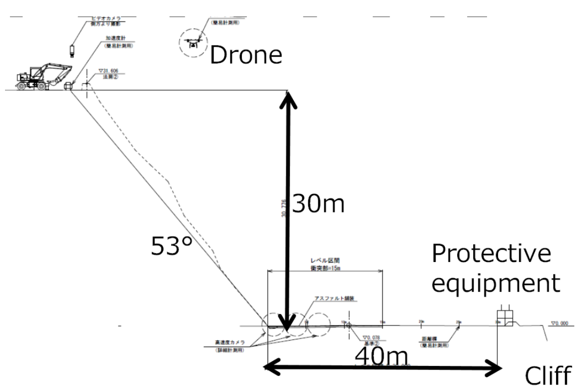


Figure 7. Cross section of Experiment

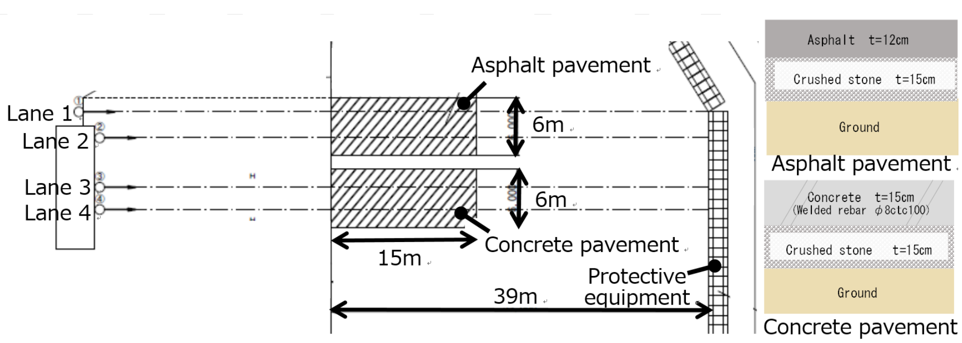


Figure 8. Plane view of Experiment

Table 1: Incident conditions (in the cross section plane)

| | Angle of incidence (°) | Incident velocity (m/s) | Rotation ratio |
|---|---|---|---|
| to asphalt(average of 20 tries) | 44.1 | 16.7 | 0.63 |
| to concrete(average of 5 tries) | 48.9 | 17.1 | 0.56 |
| total average | 45.3 | 16.8 | 0.61 |

## EXPERIMENT REPRODUCTION ANALYSIS

The specimens roll down the slope almost straight and change direction after colliding with the ground. Here, the behaviour of the test piece after colliding with the ground is reproduced. Figure 9 shows the sphere arrangement of the ground model for reproducing the experiment. Spheres of the same size as the test piece were arranged in a grid pattern at intervals of the diameter of the spheres. This arrangement is the point of the proposed model. For the collision velocity, angle and rotation ratio, the average values of the experiments shown in Table 1 were used. And the trajectory was scattered by appropriately scattering the initial position.

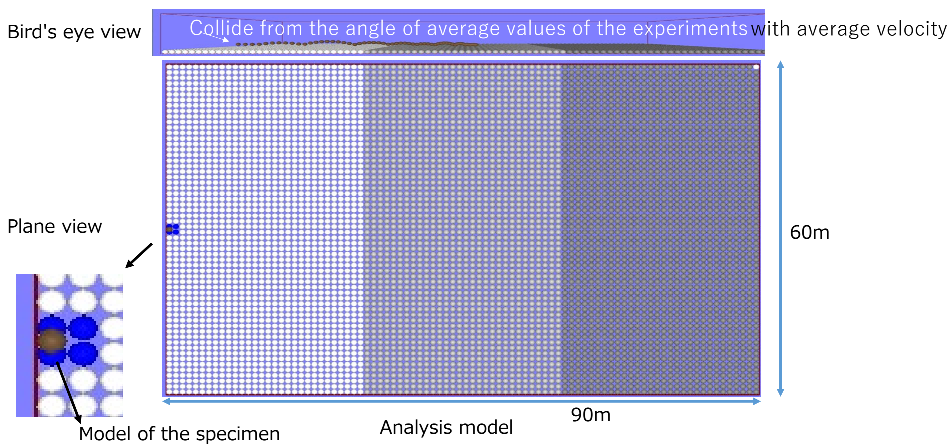


Figure 9. The model of reproduction of experiment

The simulation results with a coefficient of restitution of 0.1 are shown in Figure10 side by side with the experimental results. The figure above shows the results of the 25 experiments shown in Table 1. The x-axis represents the slope direction and the y-axis represents the slope orthogonal direction. In the experiment, the starting point was the point of fall to the ground. The black dotted line in the experimental results indicates the location of the protective equipment. The trajectory beyond the protective equipment is a predicted result. It can be said that experiments and simulations are relatively corresponding.

Since it is known that the possible range of the coefficient of restitution is 0.3 or less, we actually conducted a parametric study when the coefficient of restitution was 0.1, 0.2, and 0.3. Figure 11 shows the cumulative distribution of reach distance. The reach distance is the x-coordinate of the end of the trajectory in Figure 10. For the cumulative distribution of reach distance, the simulation error for the experiment was within about 10% in the parametric study as shown in Table2.

Table 2: Error with experiment

| Coefficient of restitution | 0.1 | 0.2 | 0.3 |
|---|---|---|---|
| Error with experiment | 10.4(%) | 7.6(%) | 8.8(%) |

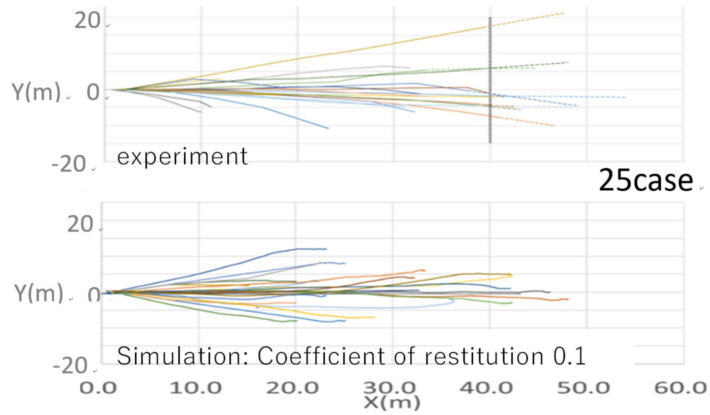


Figure 10. Comparison of experimental and simulation trajectories in plan view

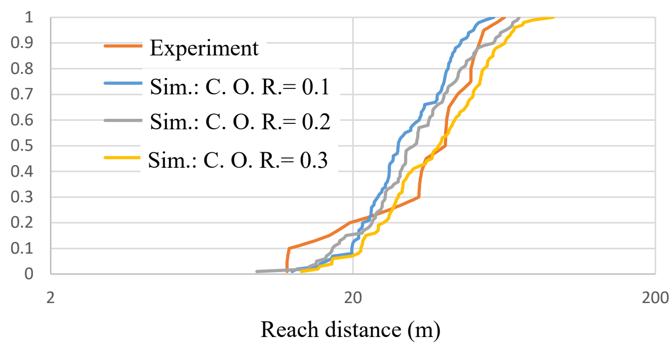


Figure 11. Comparison of experiments and simulations on the cumulative distribution of reach distance

## ANGLE OF REPOSE AND ROTATIONAL FRICTION

Suppose the slope collapses into a large number of rocks. As shown in Figure 12, when the rocks deposit on the ground, the unevenness of the individual rocks folds over each other and deposits with a relatively large angle of repose. On the other hand, if the shape is a sphere such as a DEM element, the angle of repose should be very small. We introduce rotational friction (Sakaguchi 1993) to represent a large angle of repose using a DEM element with a spherical shape. The rotational friction μr is described in reference to Figure 13. The elements are assumed to make contact with each other by surfaces and not points. A resistance F* is generated at the end of the surface with respect to the rotational moment M acting on this element, thereby generating rotational resistance Mr. The rotational friction μr is a parameter that defines size δ of the surface, which is obtained by multiplying element radius R.

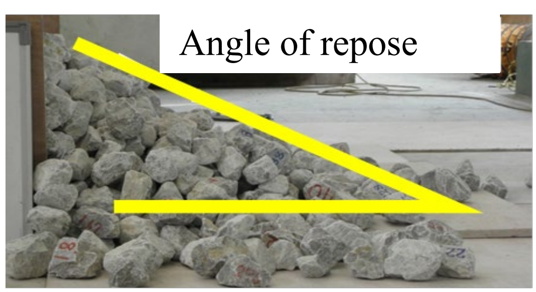


Figure 12. Angle of Repose (abbreviated as AOR)

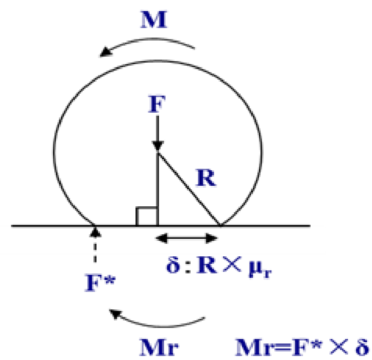


Figure 13. Conceptual diagram of the Rotational Friction (abbreviated as RF)

## LABORATORY EXPERIMENTS TO DETERMINE THE AOR

Figure 14 shows a conceptual diagram of the experimental laboratory device used to determine the AOR of various particles. After filling the particles, gradually lifting the back of the table causes the particles to spill from the edge of the cylinder, forming a conical peak. The angle of the slope of this peak is the AOR.

Figure 15 shows the experimental results for various sand and glass bead samples. The glass beads have a spherical shape, and their AOR is as small as 25°. The AOR of the sand is larger than that of the glass beads. The AOR varies between 32° to 45°, depending on the grain shape.

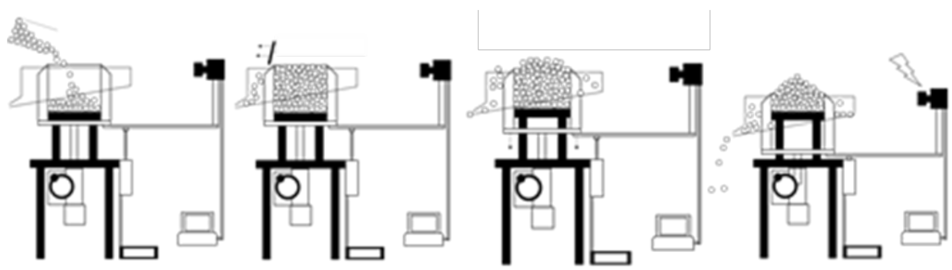

Figure 14. Conceptual diagram of the experimental laboratory to determine the AOR of various particles

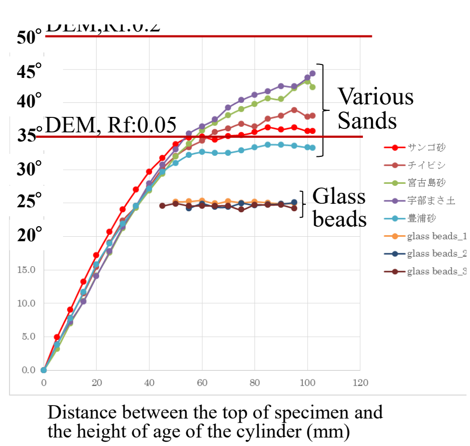


Figure 15. Experimental results

## SIMULATION OF AOR TEST

We performed a reproduction analysis of the experiment in Figure 14 using rotational friction as a parameter. The particle size was 1 cm. Particles in contact with the cylinder and those spilled out are shown in yellow-green. The remaining particles are shown in brown. Figure 16 shows the simulation results by DEM set a rotational friction of 0.05, 0.1, and 0.2. As the RF increases, the AOR increases. Figure 15 shows a AOR of 35° for a rotational friction of 0.05 and a AOR of 50° for the rotational friction of 0.2 by the red lines together with the experimental results. This shows that the AOR of sand can be expressed between RF 0.05 and 0.2.

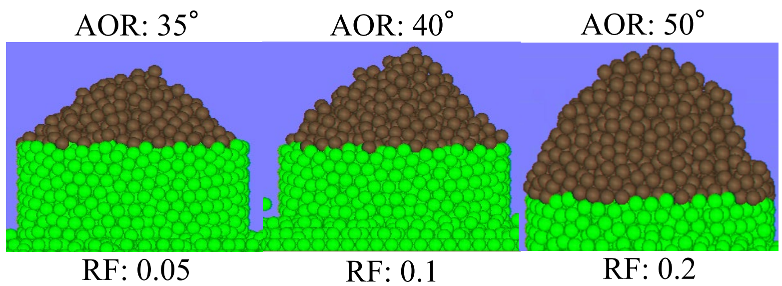


Figure 16. Simulation results

## EXAMINATION OF REPRODUCTION OF ACTUAL DAMAGE

Here, we will examine the reproduction of the actual damage shown in Figure 1. Figure 17 (a) shows a digital elevation model at 0.5 m intervals after slope collapse. The lower part of the slope shows fan-shaped deposits of collapsed sediment containing soils and rocks. Figure 17(b) shows the numerical elevation model constructed by removing the sediment containing rock mass as well as the collapsed rock shed by referencing aerial photographs and topographic maps obtained prior to the collapse. Then based on the information that the sediment deposit was 42,000 cubic meters, a model of the ground surface before the collapse was created as shown in Figure17(c). Table 3 shows the DEM analysis parameters used to construct the granular model of collapsed sediment in the simulation.

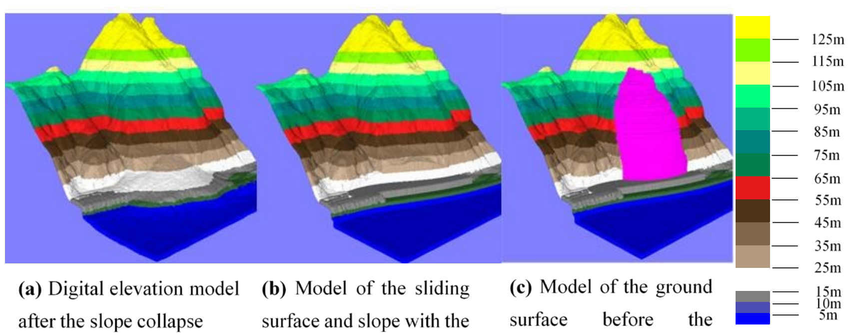


**(a)** Digital elevation model after the slope collapse

**(b)** Model of the sliding surface and slope with the sediment removed

**(c)** Model of the ground surface before the collapse (pink colored

Figure 17. Numerical elevation model after the slope collapse and for simulation

Assuming that the behaviour of rock with a relatively large diameter is dominant, the relationship between the spring constant and the damping coefficient has been adjusted so that the coefficient of restitution is 0.1. The coefficient of restitution of 0.1 is the lower limit of the possible range. We examined the values of the rotational friction in the range of 0.05 to 0.2 parametrically with reference to the examination in the previous section. As the proposed model it is allocated and set sphere elements of 2m diameter on the slope and the bottom area of non-collapsed area using the same grid coordinates at 2m intervals. The grid coordinates for the collapsed surface were in 1.0m intervals, and the friction was set to 0. DEM elements was filled between the slip surface in figure 17 and the ground surface. Then they were dropped freely in the simulation. Figure 18 shows the initial, intermediate, and reconstructed states in the simulation. Figure 19 shows the results of the parametric simulation of rotational friction. The tip of the deposit was enveloped by a part of a red circle, and the reach distance from the slope was calculated. The smaller the rolling friction, the farther the collapsed object will reach. However, the difference between the two was not so large, and it was about 9m for a slope height of 120m.

We evaluated the simulation results using the AOR for the sediment as an index. To derive the AOR for the sediment slope, we used four survey lines as shown in figure 20, line 1 to line 4. Lower part of Table 4 compares the average of AORs obtained from these four survey lines in actual damage with that of the simulation. The AOR value of the actual damage was located in the results of the parametric study conducted at RF 0.05-0.2. The AOR of RF0.175 was close to that of the actual damage. From this, it can be estimated that the reach of the actual damage deposits hidden in the sea is about 48 m.

Table 3: Parameters used for DEM simulation.

| Parameters | values |
|---|---|
| Particle diameter (m) | 2.0 |
| Density (km/m$^3$) | 2,600 |
| Spring coefficient (N/m) | $2 \times 10^6$ |
| Damping coefficient (N•s/m) | $1.74 \times 10^5$ |
| Friction coefficient (˚) | 30 |
| Rotational friction | variable |

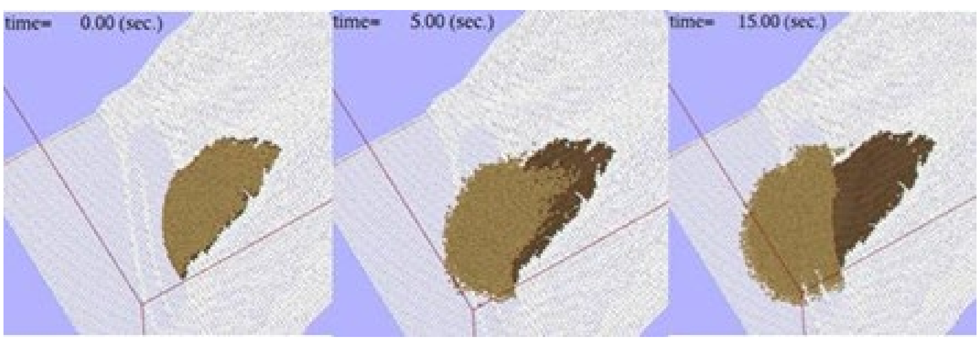


Figure 18. State of simulation

Table 4: Reach distance and angle of repose

| | DEM simulations (RF) | | | | | Actual damage |
|---|---|---|---|---|---|---|
| | 0.05 | 0.1 | 0.15 | 0.175 | 0.2 | |
| Reach distance (m) | 56 | 56 | 50 | 48 | 47 | - |
| Average of AOR(° ) | 21.8 | 21.3 | 21.8 | 26.1 | 30.1 | 27.5 |

## CONCLUSION

Even if the physical properties of the site are unknown when estimating the reach distance, it is possible to estimate the possible range of reach distance by conducting a parameter survey within the realistic range of these physical properties.

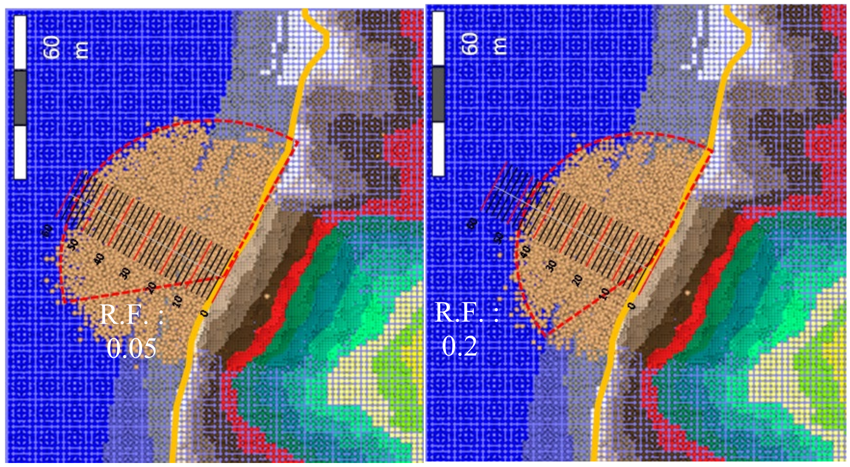


Figure 19. Result of simulation in plan view

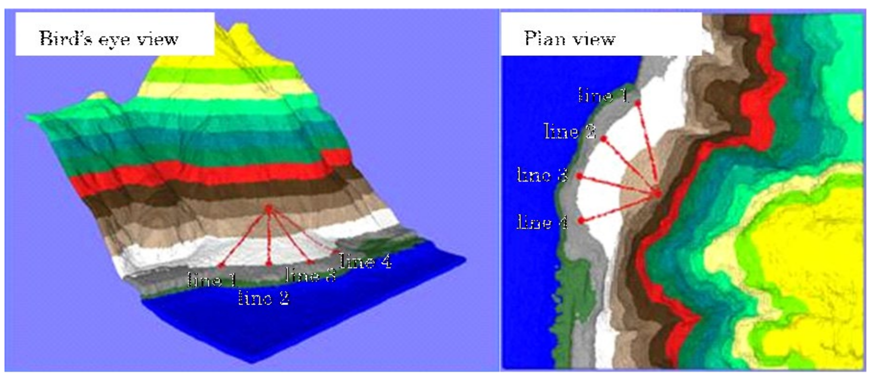


Figure 20. Survey line for finding the angle of repose

## REFERENCES

Cundall, P.A, (1971). "A Computer Model for Simulating Progressive, Large Scale Movement in Blocky Roksystem, " *symp.ISRM*, Nancy France, Proc., Vol2,pp.129-136.

Nakamura, S., Abe K., Watanabe, K., Nakajima, S. (2018)."Analysis of flow and inpulsive behavior based on existing cascading experiment of collapsed soil and reproduction analysis by MPM", *Journal of Japan Society of Civil Engineers,* Vol.74, No3, 259-274

Nakase, H., CAO, G., Tabei, K., Tochigi, H., Matsushima, T., (2015). "A Method to Assess Collision Hazard of Falling Rock Due to Slope Collapse Application of DEM on Modeling of Earthquake Triggered Slope Failure", *Journal of Japan Society of Civil Engineers, Ser. A1 (Structural Engineering & Earthquake Engineering (SE/EE))* Vol. 71,No. 4, I_476-I_492. (In Japanese)

Sakaguchi, H., Ozaki, E., Igarashi, T., (1993). "Plugging of the Flow of Granular Materials during the Discharge from a Silo," *Int. J. Mod. Phys. B*, 7, pp.1949-1963